Materials Letters 270 (2020) 127725

Contents lists available at ScienceDirect

Materials Letters

journal homepage: www.elsevier.com/locate/mlblue

Revisiting the pressure effect on carbon migration in iron

P. Maugis *, D. Kandaskalov

Aix Marseille Univ, Univ Toulon, CNRS, IM2NP, Marseille, France

ARTICLE INFO

Article history:
Received 7 December 2019
Received in revised form 6 March 2020
Accepted 25 March 2020
Available online 26 March 2020

Keywords:
Steels
Diffusion
Elasticity
Simulation and modelling

ABSTRACT

Carbon migration in bcc-iron drives the kinetics of numerous phenomena occurring during ageing of steels, such as segregation at structural defects and iron-carbide precipitation. Internal stresses are often encountered in steel microstructures and are known to affect the diffusivity of carbon. The effect of pressure on carbon diffusivity is related to the carbon migration volume. Unfortunately, theoretical and experimental studies on this migration volume are scarce and sometimes contradictory with one another. In this paper, we provide new ab initio results on carbon migration and compute the effect of an applied pressure on diffusivity. Our results are consistent with known crystallographic and relaxation data. They show that carbon diffusivity in bcc-iron can be enhanced by applying compressive pressure, a counter-intuitive and unusual effect in steels.

1. Introduction

Carbon diffusion in steel is involved in various phenomena such as segregation to structural defects, carbide precipitation and phase partitioning. A precise knowledge of carbon diffusivity in ferrite, bainite and martensite is thus essential to the development of advanced high-strength steels. The microstructure of these steels is often subjected to high internal stresses, up to a few gigapascal [1], which raises the question of the effect of such stresses on the diffusivity. However, experimental difficulties inherent to the low solubility of carbon in body-centered iron make direct measurements scarce. Hence the migration volume ΔV of carbon is largely unknown: measurements range from -0.07 to 0.0 Å^3 [2,3]. On the other hand, atomic-scale calculations of ΔV vary from -0.75 to 1.49 Å^3 [4–7]. The inaccuracy on ΔV is such that its sign itself is uncertain. As a result, one does not know whether pressure reduces ($\Delta V > 0$) or enhances ($\Delta V < 0$) the diffusivity of carbon. Besides, it is known that tetrahedral sites of the bcc crystal lattice (saddle point position for migration) are larger than the octahedral sites (stable position): a decrease of volume is thus expected during interstitial migration, *i.e.* $\Delta V < 0$. This decrease should be accompanied by an unusual accelerating effect of applied pressure on diffusion. In view of the above uncertainties and contradictions, a critical assessment is welcome, together with a detailed analysis of the migration mechanism of carbon in bcc-iron.

2. Theory and calculations

Carbon in solid solution in body-centered iron occupies the octahedral interstitial sites. Each carbon atom on an octahedral site (of type O_x, O_y or O_z) creates a prolate tetragonal distortion along the corresponding direction (x, y or z). Tetrahedral sites are unstable and occupied only temporarily as saddle points for carbon migration. A carbon atom on a tetrahedral site of type T_x, T_y of T_z creates a tetragonal distortion in the same direction (x, y or z), but of oblate character [7]. Fig. 1a illustrates a carbon jump starting from an octahedral site of type x, through a tetrahedral site of type y, and ending at an octahedral site of type z: an "x-y-z" jump. During this jump, the bcc lattice is tetragonally distorted successively along directions x, y and z.

In terms of boundary conditions applied to the crystal, two limiting cases are usually considered: (i) The stress-free crystal: insertion of a carbon atom in an interstitial site (O or T) is accompanied by a change in crystal volume called the relaxation volume V^O or V^T. During a jump, the migration volume is the difference $\Delta V = V^T - V^O$; (ii) The volume-fixed crystal: in this case, insertion of a carbon atom builds up internal stresses that have to be equilibrated by applying a stress tensor $\boldsymbol{\sigma}$ on the crystal boundary in order to maintain the volume fixed. Relaxation volumes and stresses can be computed in various interstitial configurations by atomic-scale calculations [4,6,8,9].

In the frame of the continuum elasticity theory, octahedral and tetrahedral sites are characterized by their respective defect dipole tensors $\mathbf{P}^O$ and $\mathbf{P}^T$ [10]. The corresponding migration dipole tensor is $\Delta\mathbf{P} = \mathbf{P}^T - \mathbf{P}^O$. The relaxation volume tensors are related to the

* Corresponding author.
E-mail address: philippe.maugis@im2np.fr (P. Maugis).

https://doi.org/10.1016/j.matlet.2020.127725
0167-577X/

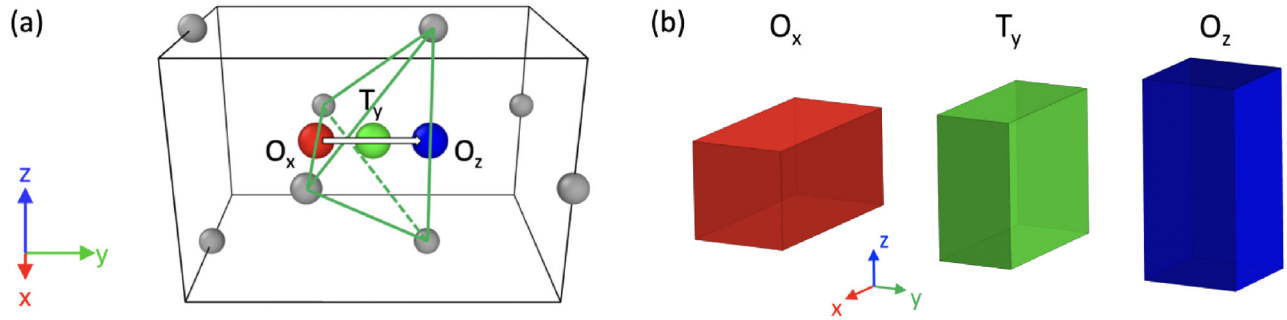

Fig. 1. (a) During an $O_x \rightarrow T_y \rightarrow O_z$ jump the carbon atom leaves the stable octahedral site O_x, passes through the saddle-point tetrahedral site T_y and ends at the stable octahedral site O_z. The atomic sites are represented by colored spheres: RGB code for *x, y, z* interstitial sites; first shell of iron atoms in grey. The co-ordinance tetrahedron of site T_y is drawn in green. (b) Schematics of the tetragonal distortions of a stress-free cell induced by the carbon atom during the successive steps of its jump. (For interpretation of the references to colour in this figure legend, the reader is referred to the web version of this article.)

dipole tensors by $\mathbf{V} = \mathbf{SP}$, where $\mathbf{S}$ is the compliance tensor of the lattice. The (scalar) relaxation volumes write

$$V^{O,T} = \mathrm{tr}\left(\mathbf{V}^{O,T}\right) = (S_{11} + 2S_{12})\mathrm{tr}\left(\mathbf{P}^{O,T}\right). \quad (1)$$

The migration volume tensor is then $\Delta\mathbf{V} = \mathbf{S}\Delta\mathbf{P}$ and the scalar migration volume writes

$$\Delta V = (S_{11} + 2S_{12})\mathrm{tr}(\Delta\mathbf{P}). \quad (2)$$

From the rate theory, the effect of pressure p on carbon diffusivity depends on the migration volume ΔV [7,11]:

$$D(p) = D(0)\exp\left(-\frac{p\Delta V}{k_B T}\right). \quad (3)$$

In this equation, $D(0)$ is the stress-free diffusivity, T is the temperature and k_B is the Boltzmann constant.

In this work, the migration dipole tensors and migration volumes were computed independently, together with the variations of energy, dipole tensor and lattice parameters along a migration path, in stress-free and in volume-fixed conditions. Volume tensors were determined from the lattice parameters a_i calculated *ab initio* via $V_{ii} = \mathscr{V}(a_i - a_0)/a_0$ where $\mathscr{V}$ is the supercell volume and a_0 is the stress-free lattice parameter of bcc-iron.

For these calculations we used the Vienna Ab-initio Simulation Package (VASP) [12] based on the density functional theory (DFT). We employed the projected-augmented wave (PAW) method [13] and the exchange–correlation functional PBE [14] with the generalized gradient (GGA) approximation. The supercell was $Fe_{128}C_1$. To calculate the dipole tensor components, ionic positions were relaxed at constant supercell shape. To study the evolution of the lattice parameters, the ionic positions and the supercell vectors were relaxed. The convergence criteria of 10^{-6} eV for total energies of ionic step iterations and 0.001 eV/Å for forces acting on the atoms have been applied. We used the nudged elastic band (NEB) method [15] to determine intermediate configurations during the minimum energy paths (MEPs). For the transition-state searches, convergence criteria of 10^{-6} eV for total energies of ionic step iterations and 0.015 eV/Å for forces acting on the atoms have been applied. We used 9 images in these NEB analyses.

Table 1
Material parameters used in the elasticity calculations.

a_0 (Å)	S_{11} (GPa^{-1})	S_{12} (GPa^{-1})	C_{11} (GPa)	C_{12} (GPa)
2.8314	6.15×10^{-3}	-2.81×10^{-3}	267	147

3. Results and discussion

For the numerical evaluations related to the elasticity theory, we used the data computed *ab initio* presented in Table 1. The NEB calculations yielded the tensors of relaxation volume of both octahedral and tetrahedral sites (in Å^3):

$$\mathbf{V}^{O_x} = \begin{pmatrix} 11.1 & 0 & 0 \\ 0 & -0.69 & 0 \\ 0 & 0 & -0.69 \end{pmatrix}, \quad \mathbf{V}^{T_y} = \begin{pmatrix} 7.17 & 0 & 0 \\ 0 & -5.32 & 0 \\ 0 & 0 & 7.17 \end{pmatrix}. \quad (4)$$

As expected, the octahedral site has a prolate character, *i.e.* the induced tetragonality of the lattice is $c/a > 1$. Conversely, the octahedral site is oblate, with $c/a < 1$. Hence, during an *x*-*y*-*z* carbon jump in the stress-free condition, the lattice is initially extended along *x* , then contracted along *y* when the carbon atom is at the saddle-point position and finally extended along *z* at the arrival site (Fig. 1b). From the volume tensors, the relaxation volumes are V^O = 9.68 Å^3 and V^T = 9.02 Å^3. It follows that the migration volume is *negative*: $\Delta V = -0.66$ Å^3. This is illustrated in Fig. 2d and 2e where the lattice parameters *a*, *b* and *c* and the change in cell volume are drawn as a function of the reaction path. The volume clearly reaches a minimum at the saddle point. This result is coherent with the crystallography of the bcc lattice: in the hard-sphere model, the tetrahedral site is approximately twice larger ($r_T \approx 0.127a_0 = 0.36$Å) than the octahedral site ($r_O \approx 0.0670a_0 = 0.19$Å). From Eshelby's theory of lattice defects [16], insertion of a carbon atom into a tetrahedral site thus produces a smaller distortion than into an octahedral site. Therefore, the crystal volume is logically reduced when the carbon atom is in the saddle-point tetrahedral site.

An alternative approach uses the formalism of defect dipole tensors. Using the residual stress method [8], we found the following values (in eV):

$$\mathbf{P}^{O_x} = \begin{pmatrix} 18.7 & 0 & 0 \\ 0 & 9.50 & 0 \\ 0 & 0 & 9.50 \end{pmatrix}, \quad \mathbf{P}^{T_y} = \begin{pmatrix} 14.7 & 0 & 0 \\ 0 & 5.32 & 0 \\ 0 & 0 & 14.7 \end{pmatrix}. \quad (5)$$

These values are close to previously published data [6,7]. They indicate that $\mathrm{tr}\left(\mathbf{P}^T - \mathbf{P}^O\right) < 0$. From the elasticity theory (Eq. (1))

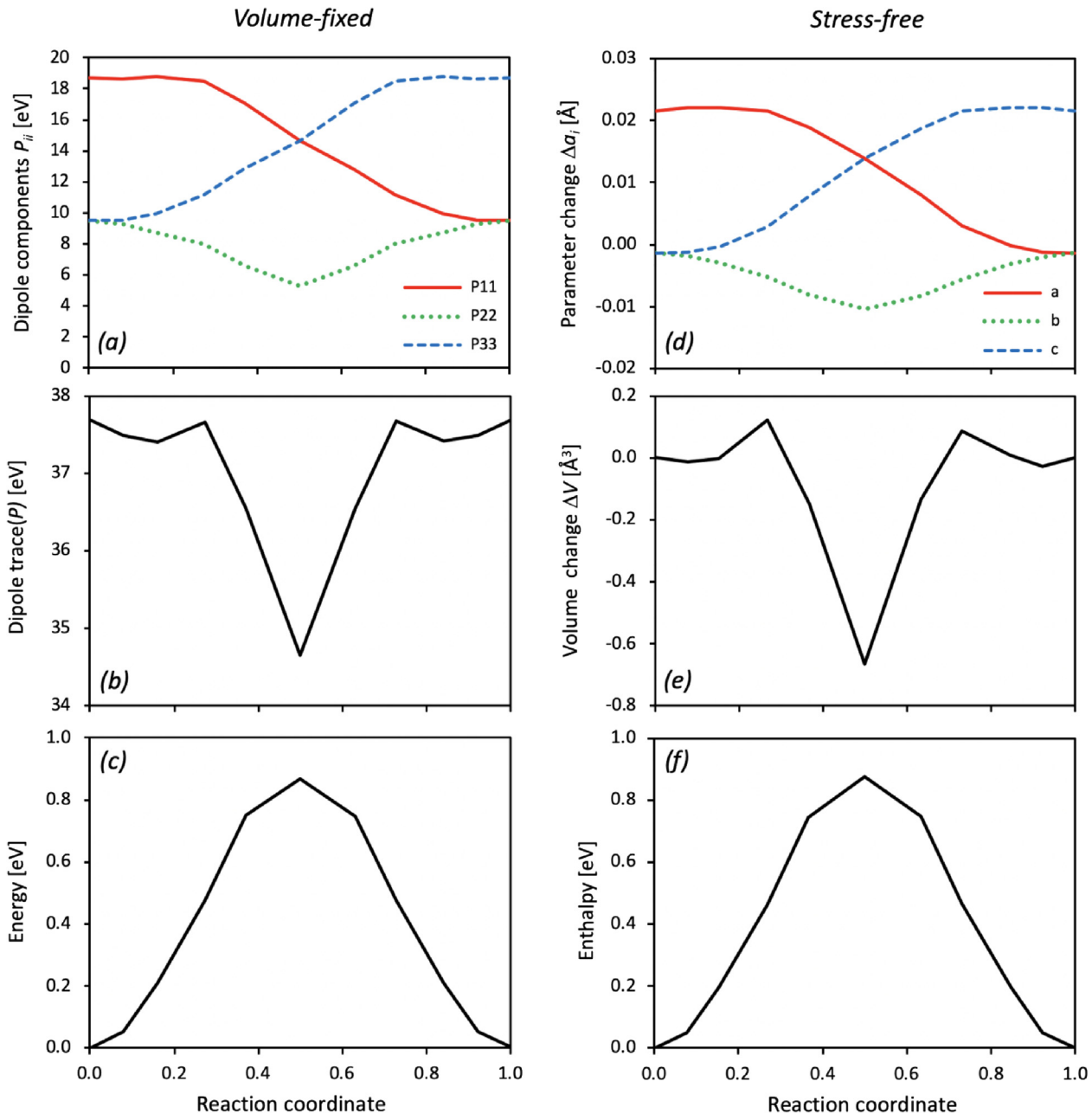

Fig. 2. DFT calculations of the migration path during an *x*-*y*-*z* carbon jump. The boundary conditions are volume-fixed (left column) or stress-free (right column). (a) dipole components, (b) trace of the dipole tensor, (c) energy change, (d) change in lattice parameters, (e) volume change and (f) enthalpy change.

the migration volume $\Delta V$is then negative, which is consistent with the direct DFT result. As expected, the variations of the components of **P** during a jump are similar to the variations of the lattice parameters and cell volume (Fig. 2a, b, d, e).

The migration energies are presented in Fig. 2c and 2f. Our migration enthalpy in the stress-free condition is H_m = 0.875 eV. This value is very close the experimental value of 0.874 eV measured in ferromagnetic ferrite (compilation of da Silva [17]) and is compatible with values computed by various techniques, ranging from 0.81 to 0.94 eV [6,18–22], see Table 2.

From the experimental data compiled by da Silva, we retrieved the pre-exponential factor D_0 = 2.24 × 10^{-6} m^2/s and migration enthalpy H_m = 0.874 eV for the diffusivity of carbon in the temperature range of −40 °C to 770 °C [17]. From Eq. (3) and our value of ΔV, the effect of pressure on the migration enthalpy is given by (H_m in eV, p in GPa):

$$H_m(p) = 0.874 - 0.0041p \quad (6)$$

The corresponding Arrhenius plots are presented in Fig. 3.

Our DFT calculations and those of Souissi *et al.* [6] yield $\Delta V < 0$. This is compatible with the available experimental data (Table 2). On the other hand, the EAM potential used by Lawrence *et al.* [4] yields $\Delta V > 0$. Hence, our results predict an increase in diffusivity with increased pressure (or decreased volume), whereas Lawrence's data predict the opposite. This difference has important consequences on the kinetics of carbon redistribution around structural defects, such as edge dislocations where the pressure is locally very high: if $\Delta V < 0$, as computed here, carbon diffuses

Table 2
Migration enthalpies and migration volumes extracted from literature data (from most recent to oldest).

	H_m (eV)	ΔV (Å^3)
This work (DFT)	0.875	−0.66
Souissi (DFT) [6]	0.871	−0.75
Lawrence (EAM) [4]		1.49
Bialon [22]	0.94	
Fors & Wahnström [21]	0.85	
Garruchet (EAM) [19]	0.81	
Domain (DFT) [23]	0.92	
Jiang & Carter (exp.) [18]	0.83	
da Silva (exp.) [17]	0.874	
Bass (exp.) [3]		0.0
Bosman (exp.) [2]		−0.07

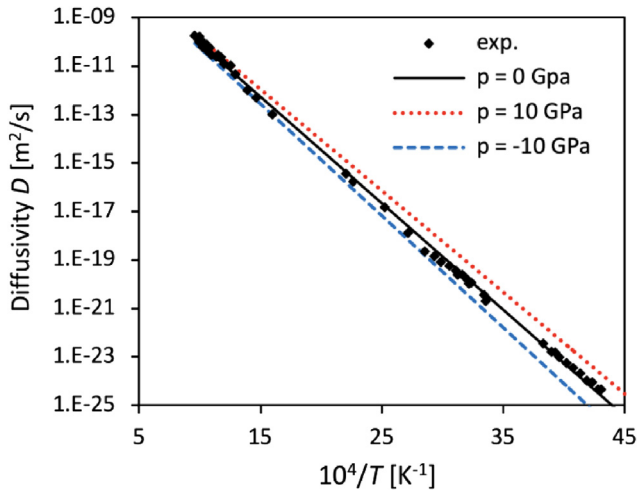

Fig. 3. Arrhenius plots of the computed carbon diffusivity under compression and depression conditions (lines) compared to the experimental results compiled by Dasilva [17] (diamonds).

faster on the compression side of the dislocation, where the equilibrium concentration of carbon is low; whereas if $\Delta V > 0$, carbon diffuses faster on the tension side, where carbon concentration is high. The diffusion flux is the product of concentration by diffusivity: in the former case, the flux of pipe diffusion in the vicinity of the dislocation will be low, whereas in the latter case, it would be much higher.

As a conclusion, linear elasticity theory of point defects applied to interstitial carbon in bcc-iron showed that carbon diffusivity is enhanced by a compressive state of stress. This result is compatible with crystallographic and diffusion data. As a consequence, pipe diffusion of carbon along edge dislocations might deserve renewed investigations.

Credit authorship contribution statement

P. Maugis: Conceptualization, Data curation, Formal analysis, Funding acquisition, Methodology, Project administration, Resources, Supervision, Validation, Visualization, Writing - review & editing. **D. Kandaskalov:** Data curation, Methodology, Resources, Writing - review & editing.

Declaration of Competing Interest

The authors declare that they have no known competing financial interests or personal relationships that could have appeared to influence the work reported in this paper.

Acknowledgement

This work was supported by the Agence Nationale de la Recherche, France (contract C-TRAM ANR-18-CE92-0021).

References

[1] M.J. Genderen, M. Isac, A. Böttger, E.J. Mittemeijer, Metall. Mater. Trans. A 28 (1997) 545–561.
[2] A.J. Bosman, P.E. Brommer, L.C.H. Eijkelenboom, C.J. Schinkel, G.W. Rathenau, Physica 26 (1960) 533–538.
[3] J. Bass, D. Lazarus, J. Phys. Chem. Solids 23 (1962) 1820–1821.
[4] B. Lawrence, C.W. Sinclair, M. Perez, Model. Simul. Mater. Sci. Eng. 22 (2014) 1–17.
[5] M. Souissi, H. Numakura, ISIJ Int. 55 (2015) 1512–1521.
[6] M. Souissi, Y. Chen, M.H.F. Sluiter, H. Numakura, Comput. Mater. Sci. 124 (2016) 249–258.
[7] P. Maugis, S. Chentouf, D. Connétable, J. Alloys Compd. 769 (2018) 1121–1131.
[8] C. Varvenne, E. Clouet, Phys. Rev. B 96 (2017) 224103.
[9] S. Chentouf, S. Cazottes, F. Danoix, M. Goune, H. Zapolsky, P. Maugis, Intermetallics 89 (2017) 92–99.
[10] R.W. Balluffi, Introduction to Elasticity Theory for Crystal Defects, Cambridge University Press, 2012.
[11] H. Mehrer, Diffusion in Solids - Fundamentals, Methods, Materials, Diffusion-Controlled Processes, Springer-Verlag, Berlin, 2007.
[12] G. Kresse, J. Hafner, Phys. Rev. B 47 (1993) 558–561.
[13] G. Kresse, D. Joubert, Phys. Rev. B 59 (1999) 1758–1775.
[14] J.P. Perdew, K. Burke, M. Ernzerhof, Phys. Rev. Lett. 78 (1997) 1396.
[15] G. Henkelman, B.P. Uberuaga, H. Jónsson, J. Chem. Phys. 113 (2000) 9901–9904.
[16] J.D. Eshelby, Solid State Phys. 3 (1956) 79–144.
[17] J.R.G. da Silva, R.B. McLellan, Mater. Sci. Eng. 26 (1976) 83–87.
[18] D.E. Jiang, E.A. Carter, Phys. Rev. B 67 (2003) 214103–214111.
[19] S. Garruchet, M. Perez, Comput. Mater. Sci. 43 (2008) 286–292.
[20] C.S. Becquart, C. Domain, J. Foct, Philos. Mag. 85 (2005) 533–540.
[21] D.H.R. Fors, G. Wahnström, Phys. Rev. B 77 (2008) 3–6.
[22] A.F. Bialon, T. Hammerschmidt, R. Drautz, Phys. Rev. B 87 (2013) 104109.
[23] C. Domain, C.S. Becquart, J. Foct, Phys. Rev. B 69 (2004) 144112–144116.